Analysis of Flow Characteristics in the Intake System of 6-Cylinder MPI CNG Engine

Seung-Hyun Ha*, Ho Young Kim**, Jin-Taek Chung**†

ABSTRACT

It has been well acknowledged that intake system plays great role in the performance of reciprocating engine. Well-designed intake system is expected to not only increase engine efficiency but also decrease engine emission, which is one of the most urgent issues in the automotive society. Thorough understanding of the flow in intake system helps great to design adequate intake system. Even though both experimental and numerical methods are used to study intake flow, numerical analysis is more widely used due to its merits in time and economy. Intake system of In-line 6-Cylinder CNG engine was chosen for the analysis. ICEM CFD HEXA was used to create 3-D structured grid and FIRE code was used for the flow analysis in the intake system. Due to the complexity of the geometry, standard $k-\varepsilon$ turbulence model was applied. Numerical analysis was performed for various inlet and outlet boundary conditions under both steady and transient flow. Inlet mass flow rate and outlet pressure variation were changing parameters with respect to engine speed. Flow parameters, such as velocity, pressure and flow distribution, were evaluated to provide adequate data of this intake system.

Key Words : CNG, MPI, Intake Manifold, Breathing Capacity, Flow Distribution, Volumetric Efficiency

1. Introduction

Increasing concern of the environment enforced every nation on strict environmental regulation. The emission regulation of the automobile which was notorious for the air pollution revised in more strict form in most nations. This trend derived the concern of the automotive society into the reduction technology of the emission. The technique has been developed in three ways, fuel technology, intake system technology and catalyst technology. Most widely, CNG is considered to have its merit in emission field which has low emission rate of CO, NOx and unburned HC. It's also a common idea that the more catalyst is used the less emission occurs. However, since catalyst is mostly composed of precious metal, more use of catalyst indicates increase of the automobile price.

Optimum design of the intake system of engine increases engine breathing capacity which indicates equal distribution of inlet flow to each cylinder and the most effective use of the inertia effect of inlet flow. In the intake system of multi-cylinder engine, complicated pulsating flow occurs due to the interference between ports. This phenomenon either increases the efficiency of the engine or decreases it. Driving this phenomenon into increase of engine breathing capacity decreases engine emission as well as increases engine

* 고려대학교 기계공학과 연소및열공학 연구실
** 고려대학교 기계공학과
† 연락저자, totoro94@korea.ac.kr

efficiency.

Various empirical and numerical methods have been undertaken for the analysis of the intake system. One-dimensional wave-action calculation code was applied to study on the transient load response of a heavy-duty turbocharged diesel engine. The transient operation was aimed at load increase from idle to full load, at constant engine speed. The response of the engine operation to several modification of engine parameters, such as valve size and timing, inlet manifold dimensions, insulation of the exhaust manifold and turbine design was evaluated.[1] For the analysis of the flow in intake parts whose volume is significant, method of characteristics was applied. Pressure wave propagation phenomena through components were numerically analyzed for different inlet pipe layouts.[2] Sung[3] applied finite difference method to analyze the flow in the intake system of 4-cylinder engine. Optimum intake chamber volume, intake pipe length and valve timing were proposed by analyzing pressure waves in the intake system. Though one dimensional methods above mentioned are frequently used due to their simplicity and reduced time for analysis, the flow in intake system is too complicated to be analyzed by one dimensional method. In most cases, one dimensional method is coupled with empirical method or only used in the early stage of engine design. The influence of the length of intake duct on volumetric efficiency and inner flow of cylinder was empirically evaluated for different engine speed, from 1000 to 3000 rpm. Three different lengths of straight duct upstream of the inlet port of the engine were considered and measurements of instantaneous mass flow rate and pressure drop across the port were reported as a function of duct length and engine speed. As resonance of the induction system was reached, significant increase of swirl velocity happened.[4] Chung et al.[5] empirically analyzed the flow characteristics in plenum chamber which was used in 4-cylinder gasoline engine. Four different plenum chamber configurations were considered to evaluate flow distribution to each port. Hwang et al.[6] numerically evaluated the response of flow characteristics in plenum chamber for different plenum chamber size. The plenum chamber was used for 4-cylinder gasoline engine and was simplified. Pressure difference between inlet and outlet was applied for the boundary condition in sine form. The overall flow field inside the intake manifold of 6-cylinder diesel engine and distribution of various quantities, such as pressure, velocity magnitude were examined by Kim et al.[7] STAR-CD, the computational fluid dynamics code, was used to show the relationship between the volumetric efficiency and inlet discharge variation in accordance with the design modification of chamber width and spacer.

This study is aimed to evaluate flow characteristics of the intake system of 6-cylinder CNG engine. The engine is under process of modification to MPI CNG engine. Due to little data of flow characteristics in intake system of engine which was originally modified from diesel engine, there exists risk of the modification. Since MPI engine provides fuel directly to intake port, unless proper amount of air flow is induced to the port, expected optimum combustion is likely to fail. It is the objective of this study to make sure that air flow is distributed equally to each cylinder by analyzing the flow characteristics in the intake system. Moreover, providing basic data for possible modification of intake system design is another objective of this study.

2. Computational Process

2.1 Governing Equation

Continuity Equation

$$\frac{\partial U_i}{\partial X_i} = 0 \tag{1}$$

Momentum Equation

$$\frac{\partial(U_iU_j + \overline{U_i'U_j'})}{\partial X_i} = -\frac{1}{\rho}\frac{\partial P}{X_i} + \nu\frac{\partial^2 U_i}{\partial X_i \partial X_j} \tag{2}$$

2.2. Turbulence Model

$k-\varepsilon$ model is used in all the simulations presented in the present paper. This model employs two additional transport equations : one for turbulence kinetic energy(k) and the other for the dissipation rate of turbulence kinetic energy(ε).

$$\frac{\partial(\rho k)}{\partial t}+\frac{1}{J}\frac{\partial}{\partial \xi^j}(\rho \tilde{u}_i k) r_i^j - \frac{1}{J}\frac{\partial}{\partial \xi^j}\left(\frac{\mu_{eff}}{\sigma_k}\frac{1}{J}\frac{\partial k}{\partial \xi^n} r_i^n\right) r_i^j = S_k \quad (3)$$

$$\frac{\partial(\rho \varepsilon)}{\partial t}+\frac{1}{J}\frac{\partial}{\partial \xi^j}(\rho \tilde{u}_i \varepsilon) r_i^j - \frac{1}{J}\frac{\partial}{\partial \xi^j}\left(\frac{\mu_{eff}}{\sigma_\varepsilon}\frac{1}{J}\frac{\partial \varepsilon}{\partial \xi^n} r_i^n\right) r_i^j = S_\varepsilon \quad (4)$$

where

$$S_k = \mu_{eff} G - \frac{2}{3}\frac{1}{J}\frac{\partial u_l}{\partial \xi^r} r_l^r \left(\frac{\mu_{eff}}{J}\frac{\partial u_l}{\partial \xi^r} r_l^r + \rho k\right) - \rho \varepsilon \quad (5)$$

$$G = \frac{1}{J}\left(\frac{\partial u_l}{\partial \xi^n} r_i^n + \frac{\partial u_i}{\partial \xi^m} r_l^m\right)\frac{1}{J}\frac{\partial u_l}{\partial \xi^n} r_i^n \quad (6)$$

$$S_\varepsilon = \frac{\varepsilon}{k}\left(C_1 \mu_{eff} G - \rho C_2 \varepsilon\right) - C_1 \frac{\varepsilon}{k}\frac{2}{3}\frac{1}{J}\frac{\partial u_l}{\partial \xi^r} r_l^r \left(\frac{\mu_{eff}}{J}\frac{\partial u_i}{\partial \xi^r} r_l^r + \rho k\right) + C_3 \rho \varepsilon \frac{1}{J}\frac{\partial u_l}{\partial \xi^r} r_l^r \quad (7)$$

The values assigned to the various empirical constants that appear in the turbulence equation are given in Table 1.

2.3. Geometry Generation and Modification

The intake system of C6AB engine shown in Figure 1 was the computational domain of the current model. The engine specification was shown in Table 2. It includes mixer, throttle body and intake manifold as shown in Figure 2. It was created with the use of CATIA, a commercial 3-D CAD programme. The throttle body was assumed to be in the state of wide open throttle for the convenience of analysis. 3-D CAD data were modified to leave only wire frame and surface data which was needed for flow analysis using same tool as shown in Figure 3.

2.4. Grid Generation

The geometry data were imported from CATIA to ICEM CFD HEXA through IGES(Initial Graphics Exchange Specification) format. Structured hexahedral grid cells were generated using ICEM CFD HEXA system. This mesh generation package generated a consistent high-quality grid. Grid density and quality were tightly controlled through the use of multi-partitioned volume, local element sizing and visual previewing of the surface mesh. About 230000 cells were generated as shown in Figure 4.

2.5. Boundary Conditions

Inlet Boundary Condition

The velocity condition and the mass flow condition were applied to inlet boundary. The turbulence kinetic energy was the square of from one to ten percent of the inlet velocity and turbulence length scale was from five to ten percent of the dominant feature, such as the hydraulic diameter of the inlet. Initial conditions used in this study were shown in Table 3.

Outlet Boundary Condition

The physical description of the pressure pulse phenomena can be initiated considering an engine cylinder coupled to an intake system which does not reflect any pressure pulse towards the cylinder. Conceptually, a single intake pipe of infinite length would fulfill this condition. In this ideal case, the pressure perturbation upstream of the valve is only dependent on the piston and valve motion. Moreover while the piston travels during the intake period, it accelerates from top dead center(TDC) to bottom dead center(BDC) and draws gas across the intake valve, producing an instantaneous reduction of pressure in the

cylinder with respect to the pressure level in the intake manifold. This pressure perturbation travels from the cylinder along the intake system toward the atmosphere. Hence, if in such conditions the instantaneous pressure evolution could be monitored, the result would be similar to that shown in Figure 5.[8] In this study, the outlet boundary condition was the pressure difference between inlet and outlet, which was assumed as sine curve as shown in Figure 6 for the period that the intake valve was open.

3. Results and Discussion

Flow characteristics and distribution were evaluated under steady condition and transient condition to provide basic data for the case of modification of intake system design.

3.1 Flow Distribution Characteristics with All Ports Open

To evaluate the validities of outlet locations of intake system, the mass flow rate ran through each outlet was analyzed with applying Neumann condition to each outlet. Velocity inlet condition for different engine speed was applied and the result was shown in Figure 7. Mass flow distribution of each outlet, outlet mass flow rate divided by inlet mass flow rate, was shown. The result of different engine speed showed similar tendency, which indicated the mass flow distribution had little thing to do with engine speed. As expected, mass flowed more to outlet 3 and outlet 4, less to outlet 2 and outlet 5 and little to outlet 1 and outlet 6 due to the inertia effect of inlet mass flow. As appeared in the Figure 7, the mass flow tended to be inclined more to left part(outlet 4, 5 and 6) of the intake manifold. Through three dimensional vector evaluation, a recirculation zone was found at the intersection of intake pipe and intake manifold, right in front of outlet 3. This recirculation leaded the inlet flow more to left part of the intake manifold. However, the difference was less than 5 percent, which indicated the mass flow distribution between left side and right side of the intake manifold was resonable.

3.2 Flow Distribution Characteristics with Two Ports Open

The 6-cylinder CNG engine has the firing order of 1-5-3-6-2-4 and valve overlap 18 Crank Angle(CA) before TDC and 50 CA after BDC, which means the great amount of period of valve overlap between ports. In 720 CA, three ports are open at the same time during total 48 CA and two ports are open simultaneously during total 672 CA and 112 CA respectively. For example, with the closure of intake port 2, the intake port 1 starts its intake period while the intake port 4 is still open. For this reason, two open outlet condition is reasonable condition which simulating real engine operating condition. Several authors[9, 10] have commented on the validity of extending steady-state testing and simulation results to the design of an actual engine where the flow process is inherently transient in nature. Although it is agreed that in-cylinder flow structures (especially tumble) are predicted less accurately by steady-state experiments and computations because the moving piston head influences flow in this region, it has been demonstrated that such results can reasonably characterize the flow mechanisms in the intake region upstream of the combustion chambers.

In Figure 8, the mass flow distributions of each outlet under two open outlet condition, outlet 1 - outlet 5, outlet 3 - outlet 6 and outlet 2 - outlet4, were shown. As expected, the closer outlet port located to inlet cylinder, the more mass flow happened through the outlet. This tendency was getting apparent as the inlet mass flow rate growed with rising of engine speed. The cases of 800 rpm and 2000 rpm showed similar results in mass flow distribution, which were a little different from the case of 1200 rpm. However the overall tendency of each case was similar, which was mostly influenced by the inertia effect of the inlet flow. Outlet 2 was shown to be fatal to the mass flow distribution in all cases, when it was open with outlet 4. The mass distribution rate of outlet 2 had less than that

of outlet 6 with outlet 3 open, which was similar case according to the layout of outlets. The recirculation zone which appeared at the intersection of inlet cylinder and intake manifold, right in front of outlet seemed to be the reason of the case.

The Evaluation was extended to real pressure condition at outlets. At 64, 184, 304, 424, 551 and 664 CA, two outlets were open with same pressure condition according to the pressure curve assumed in this study. At each engine speed, the mass flow distribution rate was analyzed in Figure 9. Case 1 was the case that outlet 1 - outlet 5, outlet 3 - outlet 6 and outlet 2 - outlet 4 are coupled. Case 2 was the case that outlet 4 - outlet 1, outlet 5 - outlet 3 and outlet 6 - outlet 2 are coupled. The result of case 1 was similar to that of Figure 8. The mass flow distribution rate didn't change much in accordance with engine speed variation and outlet 2 was still fatal to mass flow distribution. In case 2, the mass flow distribution rate of outlet 1 was worse than that of outlet 5 which was similar case according to the layout of outlets. As the engine speed went up, the mass flow distribution rate in each case tended to go up a little bit. Overall mass flow distribution rate of outlet 3 and outlet 4, where inertia effect of inlet flow was the greatest, didn't change with respect to engine speed or coupled outlet.

The average velocity distribution at each intake port was shown in Figure 10. As the engine speed growed, the average velocity difference was distinct, which resulted form the inertia effect of the inlet flow. The high velocity of inlet flow at high engine speed, which tended to flow into outlet 3 and outlet 4 due to its inertia effect, raised the velocity of outlet 3 and outlet 4.

4. Conclusion

To analyze the mass distribution of inlet flow, the intake system of 6-cylinder CNG engine was evaluated.

1. The flow characteristics in the intake system of multi-cylinder engine was evaluated, which would be used as basic data in the case of modification of intake system.

2. In the case of all ports open, the inlet flow tended to flow to the left side of the intake system. Through 3-D vector evaluation of the flow field, a recirculation was observed at the intersection of intake cylinder and intake manifold, in front of outlet 3. It seemed to be the reason that the flow wasn't distributed equally to each side of the intake system. Outlet 1 had the lowest mass distribution, while outlet 4 had the highest.

3. The velocity distribution analysis showed that the velocity difference between ports was the greatest as the engine speed rose. Outlet 3 and outlet 4 had the highest average velocity and outlet 1 and outlet 2 had the lowest average velocity. Through 3-D vector evaluation of the flow field, the velocity inside the intake system was higher in the lower part of the intake system.

4. The overall tendency of mass distribution under 2 ports open condition didn't differ much between outlet condition and pressure condition. As the engine speed rose, the mass distribution showed greater difference between port which had higher mass flow and port which had lower mass flow. This tendency was apparent comparing the results of 1200 rpm with those of 2000 rpm. Apart from the engine speed, the mass distribution rate of outlet 3 and outlet 4 didn't change much where the inertia effect of inlet flow is the greatest.

Acknowledgement

The authors wish to express their deepest gratitude to the MOE(Eco-technopia 21) for their financial support for this work.

References

[1] J. Benajes, J. M. Lujan and J. R. Serrano, " Predictive Modelling Study of the Transient Load Response in a Heavy-Duty Turbocharged Diesel Engine", SAE 2000-01-0583, 2000

[2] Massimo Capobianco, Agostino Gambarotta and Massimo Nocchi, " Unsteady Flow Phenomena and Volume Effects in Automotive Engines Manifolds", SAE 931897, 1993

[3] N. W. Sung and J. W. Song, " Flow Analysis for a Chamber Type Intake Manifold Engine", SAE 961824, 1996

[4] R. Margary, E. Nino and C. Vafidis, " The Effect of Intake Duct Length on the In-Cylinder Air Motion in a Motored Diesel Engine", SAE 900057, 1990

[5] J. W. Chung, G. H. Lee and C. S. Lee, " An Emperimental Study on the Flow Characteristics in the Plenum Chamber", SAE 99370217, 1999

[6] H. Y. Hwang, "A Theoretical Study on the Characteristics of 3-Dimensional Flow in the Plenum Chamber", Korea University, 1996

[7] M. H. Kim, I. B. Chyun, W. I. Chung, "A Study on the Flow Characteristics and Engine Performance for Geometry Modification of Intake Manifold in Six-cylinder Diesel Engine", Hyundai Motors, 1999

[8] J. Benajes, E. Reyes, J. Galindo and Jl Peidro, "Predesign Model for Intake Manifolds in Internal Combustion Engines", SAE970055, 1997

[9] Bicen A. F., Vafidis C. and Whitelaw J. H., "Steady and Unsteady Airflow through the Intake Valve of a Reciprocating Engine", ASME Journal of Fluids Engineering, Volume 107, 1981

[10] Chen A. C., Lee K., Yianeskis M. and Ganti G., "Velocity Characteristics of Steady Flow Trhough a Straight Generic Inlet Port", International Journal for Numerical Methods in Fluids, Volume 21, 1995

Table 1. Coefficients of $k-\varepsilon$ Model

σ_k	σ_ε	σ_h	C_1	C_2	C_3	C_μ
1.0	1.2	0.9	1.44	1.92	-0.37	0.09

Table 2. Specification of CNG Engine

Engine Type	4 Cycle, 6 Inline
Combustion System	SI, Lean-burn, Premixed Mixture
Bore × Stroke(mm)	130 × 140
Displacement(l)	11
Max. Torque (kg.m)	100 @ 1400rpm
Max. Power (PS)	270 @ 2200rpm
Compression Ratio	11.5
Valve Timing	18, 50, 50, 18
Air Aspiration System	Turbocharged and Intercooled

Table 3. Inlet Boundary Condition

	Velocity (m/s)	TKE*1 (m^2/s^2)	LSC*2 (m)
800 rpm	5.1168	0.2618	0.0068
1200 rpm	7.675	0.5891	0.0068
2000 rpm	12.792	1.6364	0.0068

(a) N/A Case

	Mass Flow Rate (kg/ m^2 · s)	TKE*1 (m^2/s^2)	LSC*2 (m)
800 rpm	25.761	5.08	0.0068
1200 rpm	51.614	20.67	0.0068
2000 rpm	87.769	63.7	0.0068

(b) T/A Case

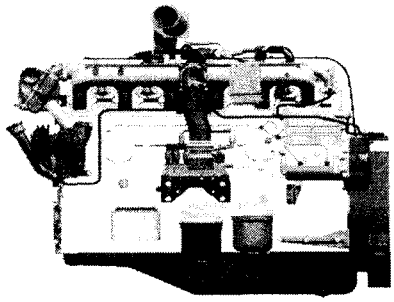

Ficture 1. Shcematic of Basic Engine

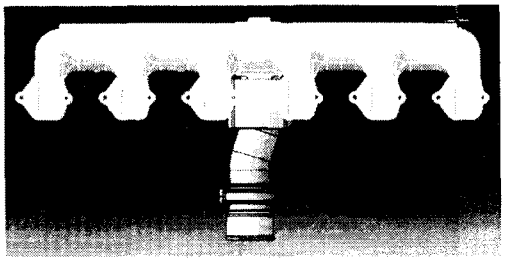

Figure 2. CAD Data of Intake System

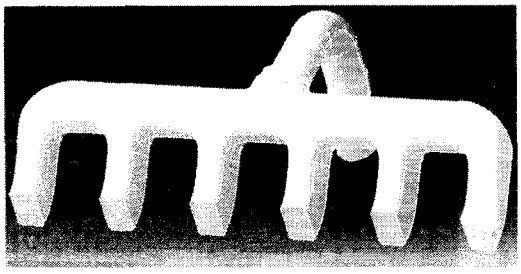

Figure 3. Surface Data of Intake System

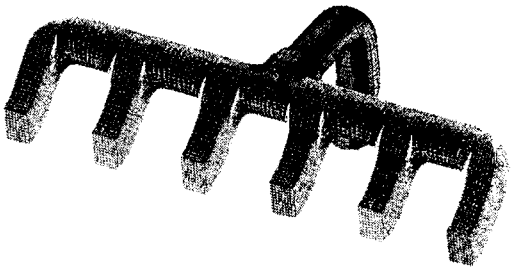

Figure 4. Grid System of Intake System

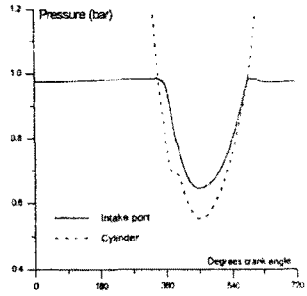

Figure 5. Wave Generated in the Cylinder

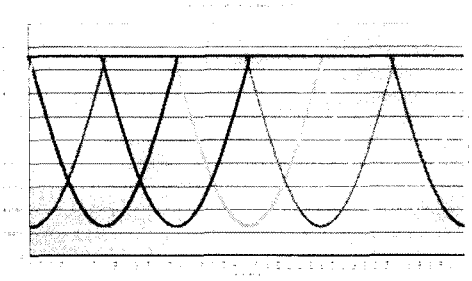

(a) 800 RPM

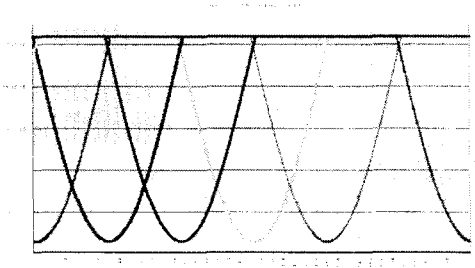

(b) 1200 RPM

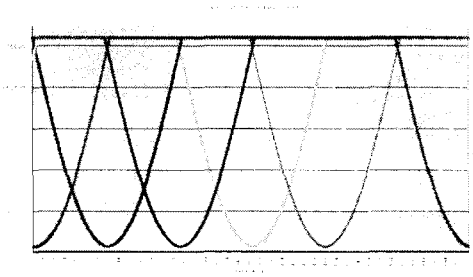

(c) 2000 RPM

Figure 6. Outlet Boundary Condition

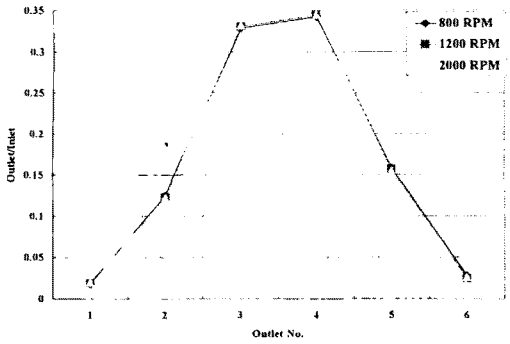

Figure 7. Mass Flow Distribution

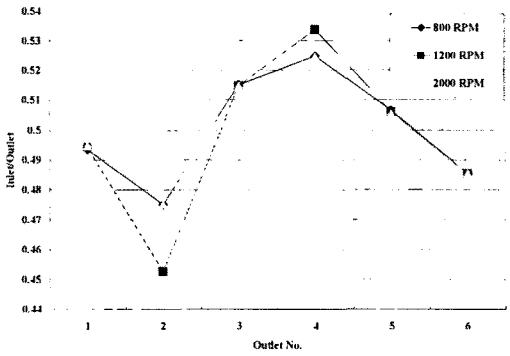

Figure 8. Mass Flow Distribution Under Two Open Outlet Condition

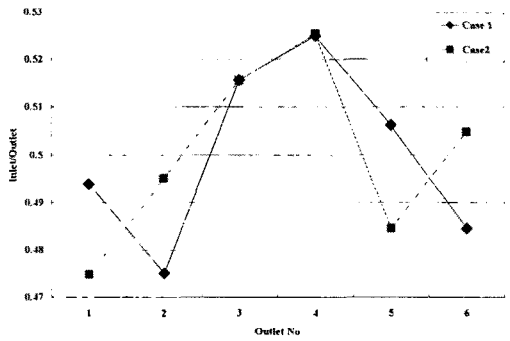

(a) 800 RPM

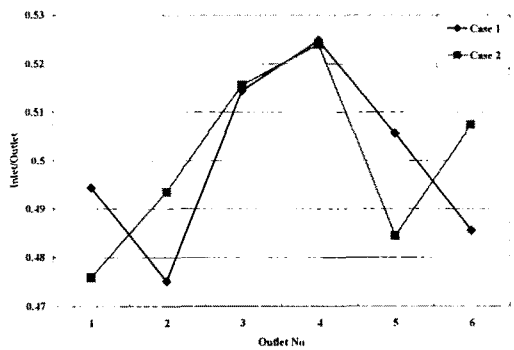

(b) 1200 RPM

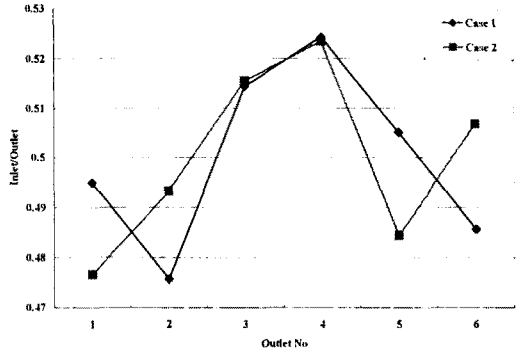

(c) 2000 RPM

Figure 9. Mass Flow Distribution Under Two Open Pressure Condition

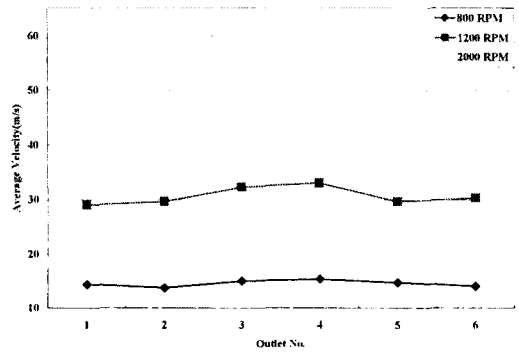

Figure 10. Average Velocity at Each Outlet